Impact of cracks on distribution of chloride-induced reinforcement corrosion

Samanta Robuschi (iD) · **Oskar Larsson Ivanov** · **Mette Geiker** · **Ignasi Fernandez** ·
Karin Lundgren

Abstract   Surface crack width is regulated in codes to limit corrosion of reinforcement bars in concrete. However, the influence of surface crack width on corrosion damages is not directly inferable from previous research. In this work, data on corroded cracked concrete specimens in chloride environments was compiled. Detailed information was included, such as crack and pit locations, local corrosion pattern, etc. Five hypotheses on the influence of transversal cracks on corrosion damage were formulated, and statistical methods were used to test them on the dataset. Transversal cracks were good indicators of the position of corrosion pits. The corrosion rate of the pit increased in proximity of a crack. With time, pits grew in depth at a slower rate but increased in number. No clear correlation between surface crack width and corrosion damage was found. Results point out discrepancies in the collected data, arguing for the need of well-defined procedures for assessing crack and corrosion damage. Further, the statistical treatment allowed for identification of bias in existing data, which was used as a research planning tool to provide guidance on the design of additional experiments. Thus, recommendations for future experimental work required to reduce the bias are given.

Keywords   Transversal cracks · Corrosion · Reinforced Concrete · Chlorides

1 Introduction

Corrosion is the most common cause of deterioration in reinforced concrete structures [1]. However, when reinforced concrete was first introduced (1853) the alkaline environment provided by the concrete medium was expected to prevent reinforcement steel from corroding. As corrosion in reinforced concrete structures is a relatively slow process, it was much later in time when doubts over the durability of reinforced concrete started to emerge [2]. Research conducted in this area in the early 1960's initially highlighted the detrimental nature of chlorides, and in the 1980s the concept of service life was introduced [3]. Consequently, new regulations were added to building codes, among others limiting surface crack width [4] and prescribing minimum concrete covers (e.g. ACI 357R-84 [5]).

In current codes and specifications, regulating maximum crack width is commonly prescribed for

S. Robuschi (✉) · I. Fernandez · K. Lundgren
Division of Structural Engineering, Chalmers University of Technology, Gothenburg, Sweden
e-mail: samanta.robuschi@chalmers.se

O. L. Ivanov
Lund University, Lund, Sweden

M. Geiker
Norvigian University of Science and Technology, Trondheim, Norway

preventing corrosion damage. To this aim, codes contain semi-empirical and empirical formulas to predict surface crack width at different loading stages. Maximum values for the allowable surface crack width are given for different exposure environments, e.g in [6] a recommanded maximum value of 0.3 mm is given for surface crack widths in non-prestressed reinforced concrete structures exposed to chloride environments. This implies that a correlation between surface crack width and corrosion damage in the reinforcing bar exists, and that an increase in surface crack width increases the probability of corrosion in the reinforcing bar. However, numerous research efforts have not been able to confirm such correlation [7–10].

Reinforcement bars are generally placed with their main direction aligned with tensile stresses appearing; accordingly, cracks will typically appear transverse to the direction of reinforcing bars. For this reason, transverse cracks are commonly in focus in studies linking surface crack widths to corrosion risk. It is generally accepted in literature that the presence of transverse cracks reduces time to reinforcement corrosion initiation [11]. This is because the cracks offer a preferential route for potentially hazardous substances, such as chlorides and carbon dioxide, to reach the reinforcing bar. Regulating surface crack width is expected to decrease the rate of ingress of deleterious species to the reinforcing bar and limit the potential negative impact of cracks on the service life of the structure. In addition the initial geometrical constrains provided by small crack widths, they also increase the probability of long-term self-healing [12].

It is recognized by numerous studies [10, 13, 14] that many other parameters have an influence on corrosion initiation and propagation, such as properties of the concrete,conditions exposure, and metallurgy of the reinforcing bars. The presence of defects and other weaknesses in the concrete may decrease the relevance of the presence of transverse cracks on the corrosion process [15]. Additionally, factors such as loading, self-healing, concrete cover and crack spacing have been observed to have an effect on the corrosion process [16–18].

An interesting aspect of the choice of limiting surface crack width is that such limitation may be contradictory with respect to the corrosion-delaying effect of the concrete cover [19]. If we look at the case of bending cracks, surface crack width increases with the concrete cover for the same crack opening at the steel-concrete interface: to decrease surface crack width, a small concrete cover may therefore be beneficial. However, increasing the depth of the concrete cover is expected to delay corrosion initiation and propagation: in the absence of cracks, it delays the transport of chlorides to the reinforcement bars through the pores. In the presence of cracks, it limits moisture variations at the rebar level and restricts the flow of oxygen to the cathodic area, thus decreasing corrosion rate [20]. In light of this, the use of performance-based limiting crack widths, i.e. adopting limits for surface crack width that vary based on other, recognized, influencing factors, such as concrete cover depth and water/binder ratio, has been advocated by many researchers [16, 21], and is even recognized by some standards [22].

This study looks into the influence of surface crack width, and the presence of transversal cracks in general, on the distribution and characteristics of corrosion damage in reinforced concrete exposed to chlorides. This was done by formulating a list of hypotheses based on literature studies. Data from studies available in literature were compiled in a dataset. It is to be noted that data included in the dataset do not come from the same experiments that the hypotheses are based on. Statistical methods were used to test the hypotheses. Finally, the statistical analysis was used as a research planning tool to provide recommendations for future experimental work required to reduce the bias in existing data.

2 Main hypotheses

In order to evaluate the influence of transverse cracks on the distribution and characteristics of corrosion damage, five hypotheses were formulated based on previous literature, especially two earlier literature reviews on this subject [11, 23]. The formulated hypotheses are supported by multiple studies and/or, a physical interpretation behind the expected influence of a certain parameter on the corrosion process.

In Table 1, the hypotheses formulated for this study are presented. For each hypothesis, the corrosion phase it refers to, as defined by Tutti [3], is highlighted. Each hypothesis is given a title, which is used through the paper to refer to it. In the following,

Table 1 Proposed hypotheses on the effect of cracks on corrosion initiation and propagation

Name	Phase	Hypothesis	Parameters
H1: Crack and pit location	Initiation	In the presence of transversal cracks, corrosion pits are more likely to form in the proximity of a crack.	P_{rate}, P_p
H2: Crack width and corrosion rate	Initiation and propagation	Corrosion rate increases with increasing crack widths for short exposure times. For longer exposure times, crack width does not influence the corrosion rate.	C_w, P_{rate}, E_t
H3: Crack width and corrosion area	Propagation	The extent of the corrosion area is independent from surface crack width.	C_w, P_t
H4: Crack width and cover	Propagation	Cover thickness and quality influences the corrosion rate more than surface crack width does.	C_w, P_{rate}, C_t, $R_{w/b}$
H5: Crack frequency and corrosion rate	Propagation	Increased crack frequency (smaller crack distances) reduces local corrosion rate.	P_{rate}, $C_{rs,m}$

a review of the sources and motivations behind each hypothesis is given.

2.1 H1: Crack and pit location

The first hypothesis states that in the presence of transversal cracks, corrosion pits are more likely to form in the proximity of a crack.

Corrosion in reinforced concrete structures exposed to chloride environments initiates with the ingress of aggressive substances through the concrete cover [24]. The decrease in corrosion initiation time due to the presence of transversal cracks has been observed in several studies and is generally accepted [13]. Once chloride ions reach the reinforcement bar, they locally break down the passive film, potentially initiating pitting corrosion if not otherwise protected. Pitting corrosion is thus expected to take place in the proximity of a crack. In the case of bending cracks, the extent of the zone surrounding the crack where pitting corrosion may take place depends as well on the length of the slip and separation zone at the steel/concrete interface in correspondence of the crack [13].

Bending is a common cause for transverse cracks, and bending cracks typically have larger crack widths at the surface than at the reinforcement level [25]. Further, the extent of the zone surrounding the bending crack where pitting corrosion may take place depends as well on the length of the slip and separation zone at the steel/concrete interface in correspondence of the crack [12]. The slip and separation developed during bending cracking and its impact on chloride ingress

and potential corrosion initiation are illustrated in [26].

2.2 H2: Crack width and corrosion rate

The second hypothesis states that corrosion rate increases with increasing crack widths for short exposure times. For longer exposure times, crack width does not influence the corrosion rate.

Large crack widths may ease transportation of chlorides through the cracks at the beginning of the corrosion period, but the effect of crack width in the long run is unclear: Schiessl and Raupach [27] observed increasing corrosion rate with increasing crack width (0.1 – 0.5 mm crack width tested) after 24 weeks, whereas no pronounced difference was observed after 2 years. They concluded that "the problem of reinforcement corrosion in crack zones cannot solely be solved by crack width limitation in the range from roughly 0.3 to 0.5 mm". Li *et al.* [28], observed the influence of surface crack width over the span of two years, and found that the highest corrosion rate consistently corresponded to the larger crack width through the entire duration of the experiments. However, in the same study, the difference in corrosion rate between specimens with different surface crack widths was observed to reduce substantially over time during the two years study. Several studies are available in literature where no dependency between corrosion rate and surface crack width was found, e.g. [4, 8, 29, 30].

2.3 H3: Crack width and corrosion area

Hypothesis three states that the extent of the corrosion area is independent from surface crack width. This hypothesis may be unexpected for some readers; it may seem natural that a larger surface crack width corresponds with larger debonding length at the steel/concrete interface, which in turn may allow for a larger area of the bar to depassivate, increasing the size of the anode and/or the number of anodes. It is interesting to observe that this, in turn, may decrease the local corrosion rate.

Many variables are expected to influence the extent of damage at the steel/concrete interface, as the crack type, the characteristics of the bond, the maximum stress reached in the steel reinforcement, and the loading history of the specimen. For this reason, several researchers have looked into the relationship between surface crack width, slip and separation at the steel/concrete interface and corresponding corrosion damage. They found that surface crack width is a poor indicator for the potential response to aggressive environment of the reinforcement bar [19], suggesting in some cases to use the maximum stress at the steel reinforcement level as a more reliable indicator of damage at the steel concrete interface [16, 31], and pointing out to debonding at the steel/concrete interface as a major influence on the corrosion extent [26, 32]. As for the loading history, cyclic loading may contribute to create additional damage at the steel-concrete interface [26].

2.4 H4: Crack width and cover

Hypothesis four states that cover thickness and quality influences the corrosion rate more than surface crack widths do. The quality of the cover depends on concrete properties, of which the water/binder ratio is generally regarded as the main influencing factor in concrete containing ordinary Portland cement.

Numerous studies have investigated the influence of cover thickness and water/binder ratio on the corrosion process, e.g. [14, 20, 33]. Scott and Alexander [34] observed a substantial decrease in corrosion rate with the increase of the concrete cover. In the same experiments, an increase in surface crack width was observed to have less substantial influence than concrete cover thickness. Schiessl and Raupach [27] observed a dependency between corrosion rate

and cover thickness, and to a minor extent, between corrosion rate and water/cement ratio. In their experiments, no relationship was observed between surface crack width and corrosion rate.

The effect of cover thickness on corrosion rate has mostly been observed in concrete containing ordinary Portland cement [14]. Otieno *et al.* [35] studied the effect of slag presence in the concrete mix, and observed that the effect of transversal cracks on corrosion rate was modified by it. Concrete samples in which a certain percentage of Portland cement was substituted with slag were less sensitive to the effect of cracking than samples without slag; i.e. the corrosion rate was not much affected by the crack width.

Finally, a decrease in water/binder ratio has been connected to an increase in concrete resistivity, a decrease in oxygen ingress, and higher alkalinity, all factors expected to decrease corrosion rate [36].

2.5 H5: Crack frequency and corrosion

The fifth hypothesis states that increased crack frequency (smaller crack distances) reduces local corrosion rate.

The hypothesis is linked to decreasing available cathode area with increasing crack frequency. Macro-cell corrosion, the process taking place in the case of pitting corrosion, relies on a large difference in size between the pit, where iron dissolves, and the cathode, where oxygen is reduced. Limited available cathode area would result in a reduction of the corrosion rate [27]. However, it is to be noted that increased crack frequency is often obtained with the use of smaller diameter reinforcement bars. Thus, it may result in higher relative loss of cross-sectional area.

2.6 Potential hypotheses not included in this work

The availability of experimental data excluded some potentially interesting hypotheses from being considered, such as the influence of mechanical loading, self-healing of the cracks, and other alternatives to replace cement than slag.

Self-healing is expected to decrease corrosion rate, and, in some cases, even repassivate the reinforcement bar. However, self-healing is rarely documented in experimental data, likely because the large bulk of available data concerns structures exposed to chloride contamination, but not to other ions typically present

in marine environment. Self-healing is mostly expected to take place in marine structures, where magnesium hydroxide and calcium carbonate may precipitate in cracks [12]. Self-healing might potentially take place also in structures exposed to de-icing salts as the source of chlorides, though in this case it is likely linked to the presence of debris, or even corrosion products, blocking the crack. Nevertheless, documentation on the latter topic is scarce.

Mechanical loading is also expected to influence the effect of transversal cracks on the corrosion rate of reinforced concrete specimens. Particularly, transversal cracks are expected to correspond to higher corrosion rate when specimens are cyclically loaded. Otieno *et al.* [35] looked into the influence of cracking and crack width in RC members by exposing 48 pre-cracked specimens to a chloride solution for 31 weeks. The crack widths varied between 0.4 and 0.7 mm, and the specimens were reloaded twice to assess the effect of crack reopening. The corrosion rate was observed to increase with the re-activation (reopening) of cracks upon reloading, and with the widening of existing cracks. Jaffer [37] studied the effect of cracks in specimens in different loading conditions (static, dynamic and unloaded), noticing higher microcell currents in cyclically loaded specimens compared to statically loaded specimens.

Mechanical loading is expected to influence the opening of surface crack widths. When loading is removed from a cracked specimen, the cracks decrease in width. Sustained load keeps the cracks open, or even increase the crack opening depending on the load magnitude. However, self-healing may close the smaller cracks. Finally, cyclic loading may contribute to removing debris and self-healing products from the crack, and even create additional damage at the steel-concrete interface [26]. No hypothesis on mechanical loading was formulated in this study, due to lack of data on the corrosion rate of cyclically loaded specimens. The type of sustained load is however still considered of interest and included among the analysed parameters, since it may influence the surface crack widths during exposure time.

3 Methodology

3.1 Experimental data collection

In order to test the hypotheses formulated in Section 2, a dataset was compiled with experimental results available in literature on the effect of transversal cracks on reinforcement corrosion in specimens exposed to chloride environments. The dataset was compiled based on a number of environmental and loading factors deemed relevant for the characterization of the corrosion process in reinforced concrete structures. Data on corrosion distribution and experimental set-ups were collected, together with data on crack location, and additional geometrical, loading, environmental and material parameters.

The following criteria were considered for selection of experiments to be included in the dataset:

- Specimens exposed to chlorides;
- Specimens that were not subjected to impressed current to accelerate the corrosion process;
- Specimens having transversal cracks;
- Specimens that were spatially documented, and where information on surface crack width and crack position were available;
- Specimens that were cracked and visually inspected after the exposure period to characterize corrosion damage in the reinforcement bars;
- Specimens for which information on the size and length of the pits were available, either as loss of cross-sectional area, maximum pit depth or surface area.

Collecting data for the dataset according to the criteria listed above proved to be challenging: the largest bulk of research on corrosion of reinforced concrete structures is carried out using impressed current to induce the corrosion process, and this was deemed as not relevant for the current study. When impressed current is used, the entire bar acts like an anode, commonly resulting in general corrosion along the entire length of the bar. Additionally, the difference in potential between anode and cathode is generally several times larger when using impressed current, compared to the natural process: this influences both spatial distribution and composition of the corrosion products [38]. For these reasons, transversal cracks cannot be expected to have a similar influence on the

corrosion process when impressed current is used as they have in real structures.

Table 2 presents the experimental campaigns included in the dataset, the source of the collected data, and the number of specimens included in the dataset from each campaign. Note that references providing the base for the main hypotheses were not included in the dataset.

3.2 Limitations

This study focused on chloride-induced corrosion; therefore the effect of transversal cracks on corrosion damage due to carbonation was not taken into account.

A limited number of studies fulfilled the criteria for being included in the dataset. This is, as described, because studies using impressed currents were not considered suitable for the purpose of this study. Further, documented observations on the extent of corrosion damage were often not described with sufficient details in available studies.

The scarce number of studies resulted in limitations on the exposure environments and source of cracks. All specimens were exposed to tap water mixed with chlorides; the dataset is therefore representative for structures exposed to de-icing salts. However, since the type of exposure solution is expected to influence the self-healing mechanisms [12], the dataset is not fully representative for structures exposed to marine environments. Specifically, the presence of magnesium and sulphate ions in sea water can lead to the precipitation of brucite and ettringite. In experiments with tap water, the precipitation of calcite is instead observed [63].

Similarly, all of the specimens were pre-cracked in 3-point bending before exposure. Bending cracks typically have a triangular shape, i.e. they are larger at the concrete surface than they are at the steel/concrete interface. Other types of cracks have different shapes and morphologies. The same surface crack width could therefore correspond to a different crack opening at the steel/concrete interface, depending on the origin of the crack. These aspects should be taken into account, if the findings from this study are to be generalised.

Moreover, depending on the length of the exposure period, many specimens included in the dataset also had corrosion-induced cracks. Corrosion-induced cracks, by increasing the availability of oxygen, as well as by giving further access to the reinforcement bar to aggressive substances, are expected to increase the corrosion rate. They may also cause a more generalised type of corrosion [8, 45].

Additionally, not all factors that are expected to influence the corrosion process could be included in the dataset, due to lack of availability of data. Examples of such factors are concrete resistivity, steel metallurgy, and slip and separation at the steel/concrete interface in correspondence of the crack. Furthermore, various authors measured parameters, such as pit characteristics and crack morphology, in different ways. In some cases, this resulted in non-comparable measurements, and, consequently, the dataset needed to be divided in subsets to allow for analysing the dataset using statistical methods.

3.3 Overview of the dataset

The dataset used to test the hypotheses contains 62 specimens, with a total of 133 reinforcement bars (total length 201.4 m), 306 cracks, and 1198 pits. Information on each sample, crack and pit is collected in the dataset. The entries in the dataset can be divided in two main groups: experiment configuration

Table 2 Experimental data included in the dataset

Experimental campaign	Information source	Number of specimens	Exposure time	Exposure environment
Jaffer, University of Waterloo (CA)	[37]	36	18 months	3% NaCl, wet/dry cycles, specimen partially submerged in chloride solution in the wet phase
Francois et al., University of Toulouse	[20, 39–61]	19	27 months - 28 years	3.5% NaCl, spraying (salt fog), continuous or in cycles
Chen et al., Chalmers University of Technology	[8, 62]	5	36 months	16.5% NaCl, wet/dry cycles

parameters, i.e. characteristics of the specimens decided at the design of the experimental campaigns, such as water/binder ratio and cover thickness; and result data, such as pit depth and position. Below, the content of each group is presented, together with an overview of their variation through the collected data.

3.3.1 Experimental configuration parameters

Experimental configuration parameters depend on experimental choices and their correlation may indicate the presence of biases in the dataset. The main experimental configuration parameters were identified as:

- Chloride concentration ($R_{Cl,}$): percentage of chlorides in the environment surrounding the specimen;
- Water/binder ratio ($R_{w/b}$);
- Type of mechanical loading (L_t): the specimens in the dataset were either unloaded, loaded statically, or cyclically during exposure. All the specimens were pre-cracked before exposure, therefore the loading condition refers to the loading status under the exposure time. In the dataset, a number from 1 to 3 was assigned to the specimen depending on the loading condition (in order from 1 to 3: unloaded, static, and cyclic);
- Exposure time (E_t): the time from the initial exposure of the specimen to the chloride environment to the end of the experimental campaign, measured in months;
- Bar diameter (D_{bar}), expressed in mm;
- Cover thickness (C_t), expressed in mm. It was defined as the shortest distance between the bar and the surface of the specimen exposed to chloride contamination;
- Percentage of slag (R_{slag}): the percentage of slag replacing Portland cement in the concrete mix;
- Average crack spacing ($C_{rs,m}$): average distance between cracks in a tested specimen, expressed in mm.
- Crack width (C_w): the width of each crack at the concrete surface in mm. Crack width was defined at the beginning of the exposure time if more than one measurement was available. It should be noted that surface crack width was measured in different ways in the different studies; For e.g. the height of the cross-section at which the measurement was

taken, the number of measurements taken per crack and the time of measurement, etc.;
- Number of cracks (N_{cracks}): total number of cracks per meter of bar;
- Crack position (C_p): expressed in mm and measured along the length of the specimen;
- Presence of corrosion-induced cracks.

In Fig. 1, an overview of the characteristics of the specimens included in the dataset is given. The chloride concentration in the environment surrounding the specimens varied between experimental campaigns: Francois et al. used a solution with 3.5 % of chlorides, Jaffer used 3 %, and Chen et al. considered 16.5 %. Water/binder ratio varied between 0.35 and 0.5, and exposure time ranged from 18 months to 27 years (see also 2).

Concrete cover varied between a minimum of 16 mm and a maximum of 48 mm, with bar diameter varying between 6 and 16 mm. Most of the specimens were made with Portland cement, but in some specimens from Jaffer [37], 25 % of the Portland cement was replaced with slag. Finally, an overview of minimum and maximum crack width in the specimens is given.

In Fig. 2, an overview of the crack characteristics along the dataset is given. It should be noted that a significant portion of the dataset contained specimens with corrosion-induced cracks. Corrosion pits, being connected to local breakdowns of the passive film, are expected to form prior the formation of such corrosion-induced cracks. Still, only information on the corrosion pits was included in the dataset, such as pit position, length, and depth. General corrosion was thus not included.

In Fig. 2, it is also important to observe the distribution of crack width: a significant part of the cracks has an opening smaller than 0.3 mm, which is the limit for surface crack widths in chloride environments prescribed by the codes [6].

3.3.2 Result data

Result data refers to individual measurements of pits morphology and calculated average corrosion rate. Specifically, the following parameters are listed in the dataset:

Fig. 1 Overview of experiment parameters and crack widths in the dataset. Note that ranges in the histograms are defined as inclusive on left, and exclusive on the right, with the exception of the last range, that is as well inclusive on the left
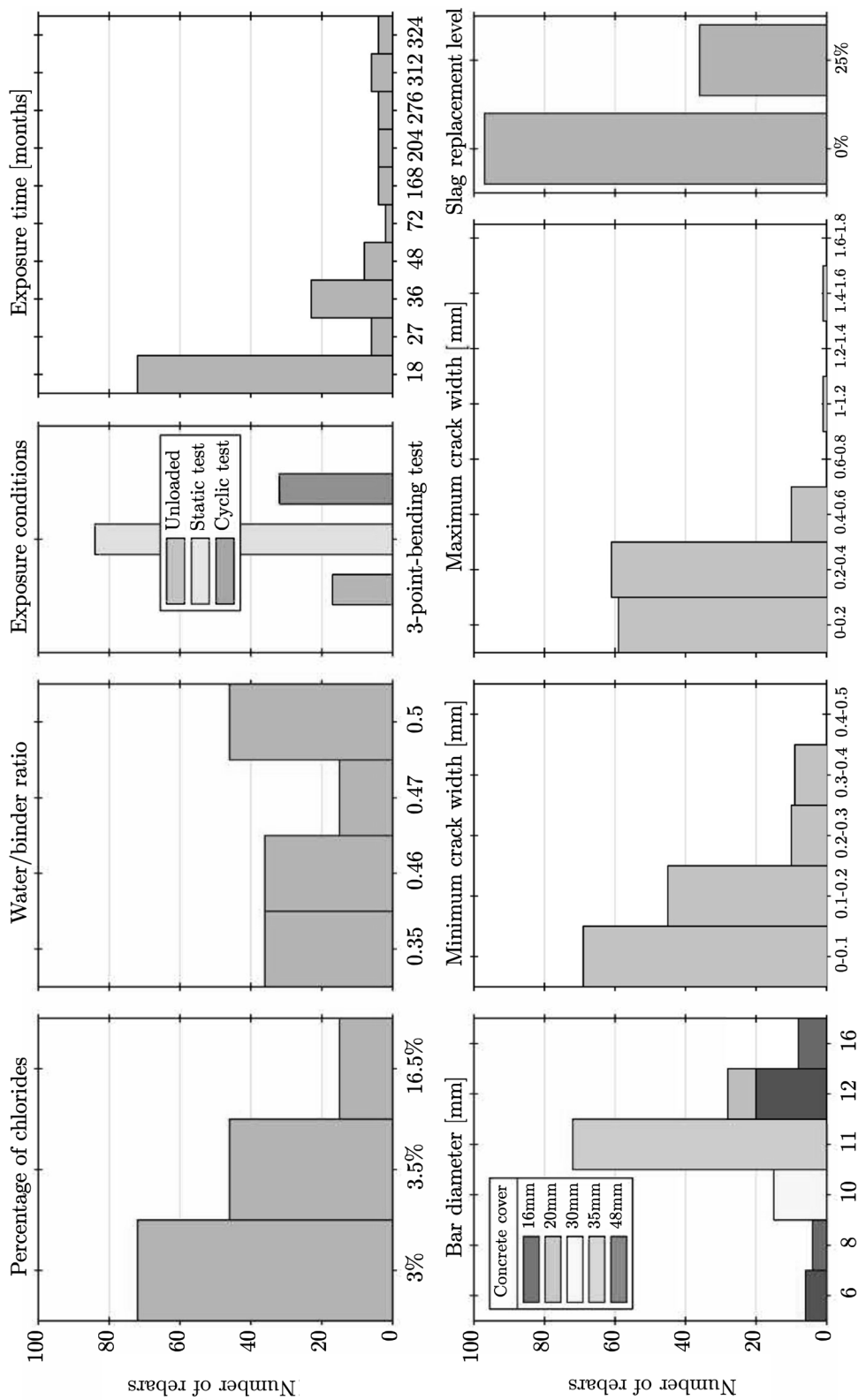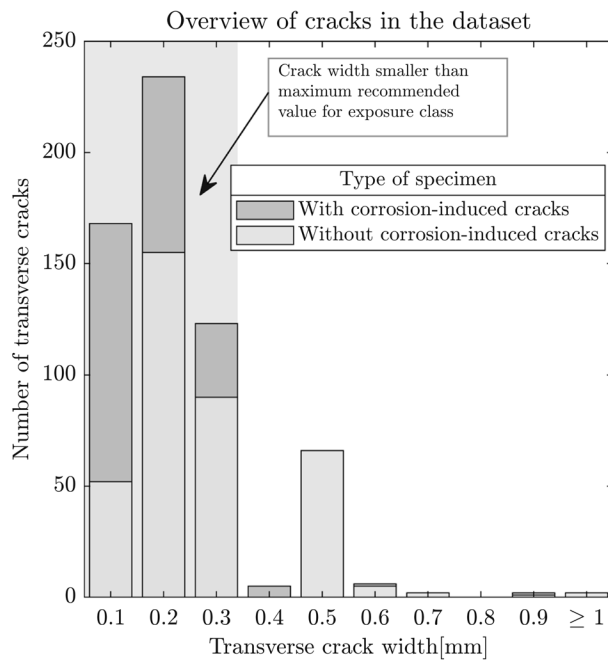
Fig. 2 Overview of cracks across the dataset

- Number of pits (N_{pits}): the number of pits per meter of bar.
- Pit position (P_p), in mm: the distance between a pit and its closest crack;
- Pit length (P_l), defined as the length of a corrosion pit on the reinforcement bar, in mm;
- Pit surface area (P_{surf}): the surface area of a pit on the reinforcement bar, in mm^2;
- Pit loss of cross-sectional area ($P_{c,area}$), defined as the maximum loss of cross-sectional area at a pit, and in mm^2;
- Pit depth ($P_{c,depth}$): measured in correspondence of the maximum depth of the pit, in mm;
- Average pit corrosion rate (P_{rate}): maximum depth (or loss of cross-sectional area) of a pit divided by the total exposure time of the specimen. This is not to be confused with the actual corrosion rate; the speed at which the reinforcement bar deteriorates at a given time. The actual corrosion rate cannot be calculated without knowing the actual period of active corrosion, and it is expected to be highly dependent on local conditions and to vary in time. The period of active corrosion is not exactly equivalent to the exposure time due to an expected time to corrosion initiation. In one of the studies, many of the specimens showed active corrosion after a period between 1 and 10 days from the beginning of the exposure period [64]. In this case, considering the period of active corrosion equal to the total exposure time may lead only to a negligible error. However, in a different study, the initiation phase for the specimens exposed for the longest period of time (27 years) was estimated to 4.5 years [65], though the estimation was based on the time necessary for corrosion-induced cracking to take place.

Not all specimens included in the dataset had information available for every parameter. Also, not all available information was directly comparable. Particularly, pit size was measured differently in various studies. The largest part of the dataset defined corrosion damage as maximum loss of cross-sectional area, while a significant part of it used pit depth to classify corrosion pits, and a smaller part of it measured pit surface area. Each type of measurement was treated individually and considered not comparable to the other ones. The same applies to measurements of average corrosion rate, which were based on pit growth measurements.

3.4 Statistical methods

In order to test the hypotheses formulated in Sect. 2, statistical methods were applied to the collected data. Specifically, the probability of a linear or monotonous relationship between the collected parameters was studied, using Pearson's and Spearman's correlation coefficient. The methodology used is briefly summarized in the following section.

3.4.1 Data treatment

The collection of data included obtaining information from tables, graphs and images of the analysed specimens, and data was stored in an object oriented dataset. A combination of the software MATLAB and the programming language R was used to store and analyse data.

The first statistical test applied to the data was the calculation of Pearson's correlation coefficient (Pearson's r) [66, 67]. Pearson's correlation coefficient is a measure of linear correlation between two sets of data; the closer to 1 is the absolute value, the likelier it is that a linear relation exists between the two sets of variables. A condition to calculate Pearson's r is that

both variables should be normally distributed [68]. The skewness in the distribution of each parameter was checked to assure that the normal distribution condition was satisfied. This, however, was not the case for many variables in the dataset. To calculate the Pearson's r, each variable was therefore first transformed into a normally distributed variable. This was done by applying a box cox transformation [69]. Following the box cox transformation, the values in the variable were as well normalized. This was done to avoid problems with values having drastically different scales.

Together with the Pearson's r, the statistical significance of the test was calculated, expressed as a p-value between 0 and 1. The statistical significance of the test tells us if what is observed in the sample is expected to be true in the population. The p-value is the probability of obtaining the data observed in the dataset, being the null-hypothesis true. The null-hypothesis is the hypothesis that there is no significant relationship between the two variables; any observed correlation being due to sampling or experimental errors. If the p-value is measured e.g. equal to 0.05, there is a 5 % chance to obtain the results currently in the sample in a world where the null-hypothesis (no correlation) is true. The lower the p-value, the higher the significance of the observed correlation. In this work, a significance level of 5 % was used as threshold, and two variables having a p-value greater than 0.05 were considered uncorrelated.

Another coefficient used in this work is Spearman's rank correlation coefficient (ρ), which measures the strength and direction of a monotonic association between two variables [70]. If the relationship between two variables can be perfectly represented by a monotonous function, ρ assumes an absolute value equal to 1. The sign, positive or negative, indicates the sign of the correlation. The main difference between Pearson's and Spearman's coefficient is that the first assesses linear relationships, while the second assesses monotonic relationships. An additional difference is that Pearson's r works with the normalized data values of the variables, whereas Spearman's ρ works with rank-ordered variables. The same significance level of 0.05 was used for both coefficients.

In the work presented in this paper, Pearson's and Spearman's coefficients are used for different purposes. When experimental choices are compared, the Pearson's coefficient is used. Experimental choices are compared in order to look for possible biases in the dataset, and the presence of a linear relationship between two experimental parameters is a clear sign of possible biases. The Spearman's coefficient is used to test the hypotheses on the collected data: in this case, the presence of a monotonic trend between an experimental parameter and a certain characteristic of the corrosion pits would indicate that the experimental parameter influences the corrosion process. The influence of the parameters is not expected to be linear.

4 Results and discussion

4.1 Presentation of the results

The relationship between the five hypotheses formulated in Section 2 and the collected dataset was analysed using statistical methods. To do so, the likeliness of a linear or monotonic correlation between the main parameters in the hypotheses formulation was calculated.

Each statistical analysis is presented in the form of a table, where the Spearman's coefficient between the parameters of interest is presented. For each couple of parameters, the value of the Spearman's coefficient is indicated by a colour, following the scale below the figure, where the colour blue represents positive correlation and the colour red represents negative correlation. The size of the circle relates with the size of the absolute value of the Spearman's coefficient: the larger the circle, the higher the likeliness of the existence of a monotonic relation between the parameters. Blank cells indicate a p-value larger than 0.05, meaning that there is a probability higher than 5% that the observed data have occurred due to chance in a scenario where the null-hypothesis (no correlation) is true, i.e. the two parameters are not likely to be correlated. All statistical analyses in this work are displayed in this format.

4.2 Correlation between experimental configuration parameters

From the analysis of the hypotheses, it was evident that correlations between choices made in the design of the experiments influenced the results of the study.
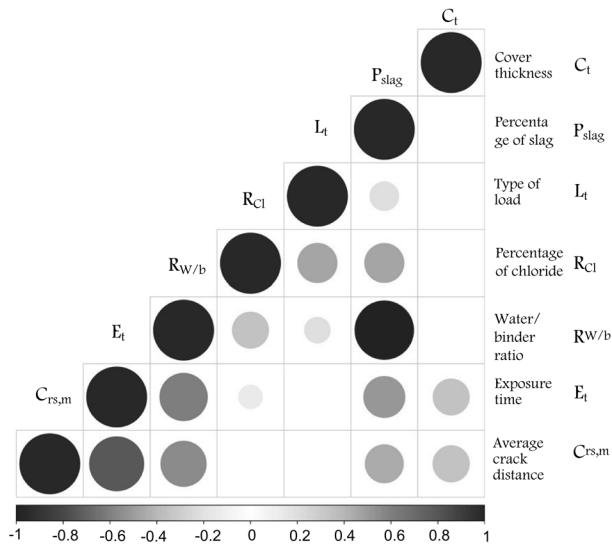
Fig. 3 Representation of the Pearson's r between variables chosen in the design of the experiments in the dataset. Blank cells correspond to p-values larger than 0.05. Note that the size of the circles increases with the absolute values of r

This is partially due to the limited number of studies included in the dataset.

In Fig. 3, the Pearson's r was calculated between experimental parameters in all experiments included in the study. Observed correlations are described in the following:

- The exposure time (E_t) is strongly correlated with many experimental choices in the dataset. Given that corrosion rates where calculated from the time, this introduced a bias in the dataset, that made it difficult to interpret correlations between corrosion rate and other parameters.

- Cover thickness (C_t) varies between 16 mm and 46 mm in the presented dataset (see Fig.1). It is positively correlated with exposure time (E_t),and average crack spacing ($C_{rs,m}$). Studies with larger concrete cover values are scarce. Increasing crack distance is expected to increase local corrosion rate, while increasing cover thickness is expected to decrease it.

- P_{slag} is negatively correlated with $R_{w/b}$. This means that slag was used as a substitute for part of the cement only in concrete of higher quality. Both the presence of slag and low water/binder ratio are expected to decrease corrosion rate, but may increase the relative effect of transversal cracks [37].

- L_t shows negative correlation with the percentage of chlorides (R_{cl}). Thus, unloaded specimens were exposed to higher percentage of chlorides. The two factors may counteract each other in short-term experiments, as a higher percentage of chlorides is expected to decrease the initiation time, but cycling loading should favour penetration of chlorides in cracks.

- Water/binder ratio ($R_{w/b}$) varies between 0.35 and 0.5, and was positively correlated to exposure time (E_t) and average crack spacing ($C_{rs,m}$). An increase in average crack spacing is expected to increase corrosion rate, and a decrease in water/binder ratio is expected to increase the influence of cracks on the corrosion distribution.

4.3 H1: Crack and pit location

Hypothesis 1 says in the presence of transversal cracks, corrosion pits are more likely to form in the proximity of a crack. Therefore, the main parameter involved in this hypothesis is the location of the pits with respect to the location of the closest cracks (P_p). This hypothesis was mainly analysed by observing how the collected data were distributed: in Fig. 4, the distance between each crack and the closest pit is shown, normalized by the spacing between the two cracks enclosing the pit. Thus, this ratio is relevant only when smaller than 0.5; else the pit is considered to belong to the influence area of the neighbouring crack.

Two different cases are presented: specimens with and without corrosion-induced cracks. In both cases, pits were observed to typically appear close to a transversal crack. Not all cracks were observed to have a corresponding pit in their proximity: the presence of corrosion at a certain crack, however, may electrochemically protect the rebar close to that spot, preventing corrosion from taking place at neighbouring cracks, as described by [71]. When corrosion-induced cracks were present, the results showed that the likeliness of corrosion at the crack increased (compare Figs. 4 a and b). This was considered to be a reasonable result, as the corrosion-induced cracks were signs of corrosion, and also due to that these rebars likely were further into the corrosion propagation phase.

Fig. 4 Distance between transversal cracks and the closest pit, averaged by crack spacing. Specimens without corrosion-induced cracks (top). Specimens with corrosion-induced cracks (bottom)
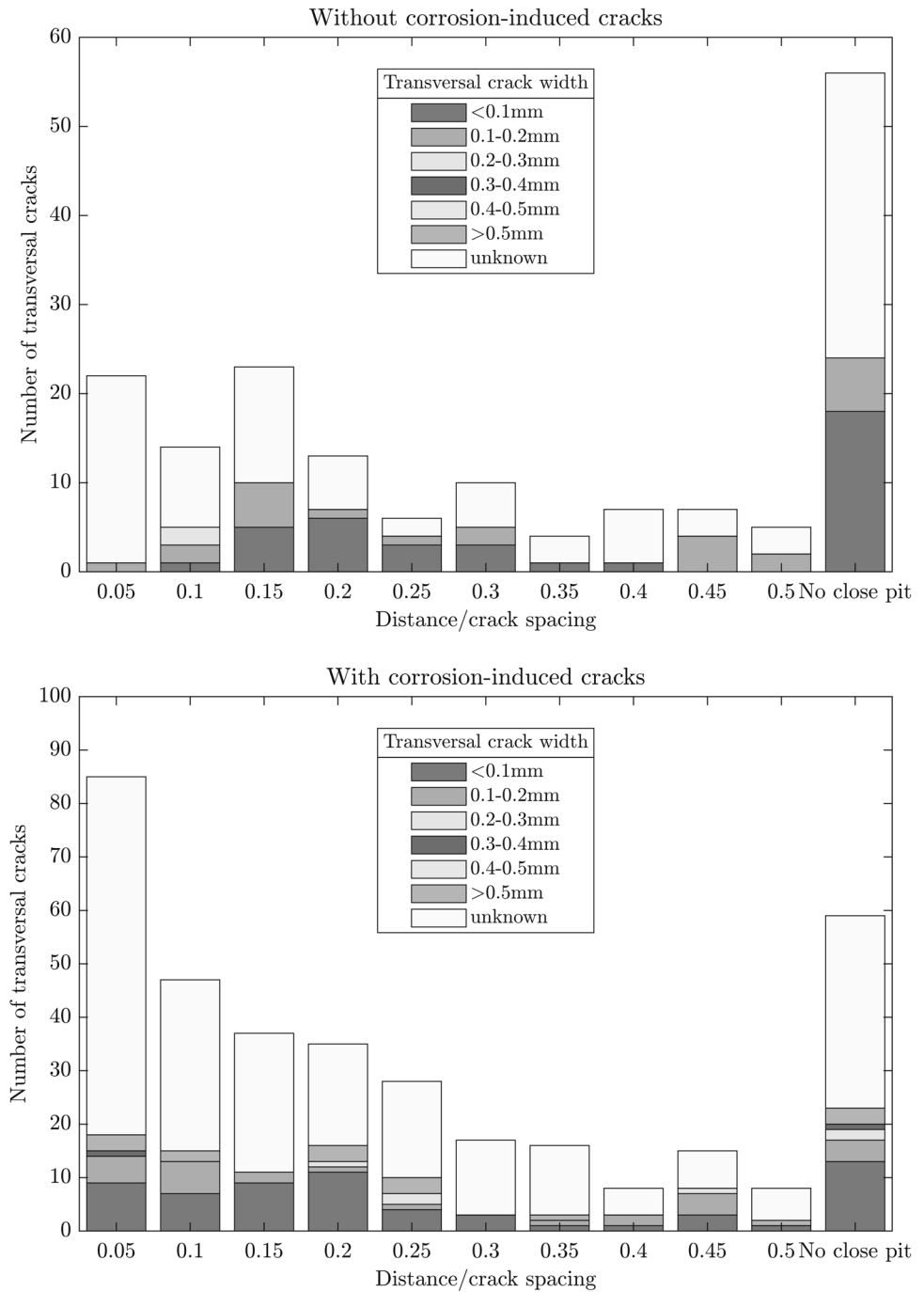
Both Figs. 5 and 6 could be used to further look into **H1**. In Fig. 5, corrosion rate is calculated from the loss of cross-sectional area, while from the maximum pit depth in Fig. 6. It should be noted that Figs. 5 and 6 show results from two different subsets of data, as the local corrosion level was measured in different ways in different studies. By looking at the relationship between the distance between a pit and its closest crack (P_p) and corrosion rate (P_{rate}), it could be observed if the distance to the crack affects the corrosion rate of the pit. In both figures, P_p and P_{rate} were observed to have a negative correlation; implying that pits further away from a crack have lower corrosion rate than pits closer to a crack. It can be noted that the absolute value of the Spearman's coefficient varies between the two figures, with the correlation being weak in Fig. 5, and stronger in Fig. 6. The relationship between exposure time and pit
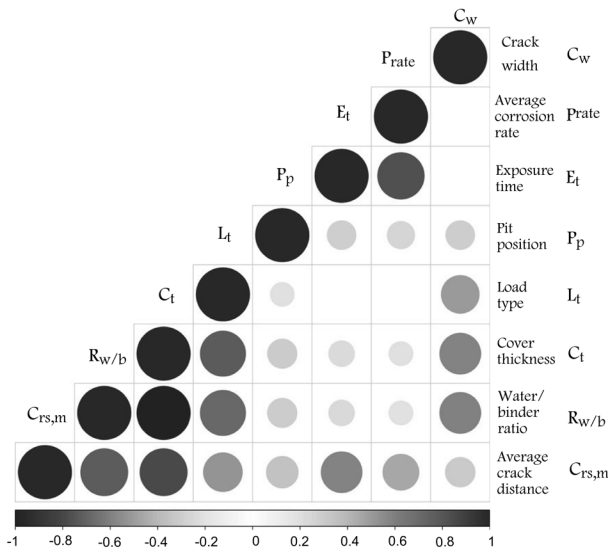
Fig. 5 Representation of the Spearman's coefficient between main parameters in an extract of the dataset in which corrosion rate is calculated as the ratio between loss of cross sectional area and exposure time. Blank cells correspond to p-values larger than 0.05. Note that the size of the circles increases with the absolute values of ρ
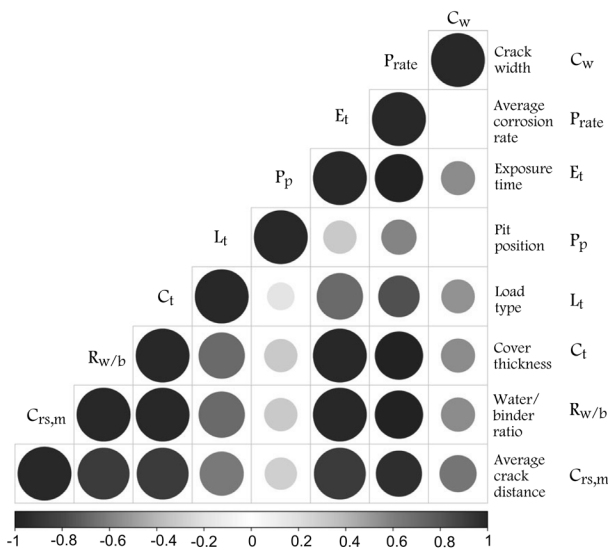

Fig. 6 Representation of the Spearman's coefficient between between main parameters in an extract of the dataset in which corrosion rate is calculated as the ratio between maximum pith depth and exposure time. Blank cells correspond to p-values larger than 0.05. Note that the size of the circles increases with the absolute values of ρ

position may influence this observation. A positive correlation between E_t and P_p indicates that additional corrosion pits form further away from the crack with increasing exposure time. This may be linked to a higher chloride concentration in the concrete with

time. Further, the formation of corrosion-induced cracks likely influences the distribution and formation of additional pits. However, the correlation is weak: this may be related to the limited variation in exposure time of the specimens, especially to the scarce availability of experiments with a length between 5 and 10 years.

4.4 H2: Crack width and corrosion rate

The second hypothesis says corrosion rate increases with increasing crack widths for short exposure times. For longer exposure times, crack width does not influence the corrosion rate. Thus, we investigate the correlation between corrosion rate (P_{rate}) and crack width (C_w), considering also the exposure time (E_t) to define short and long time studies. To support **H2**, the dataset should show positive correlation between C_w and P_{rate} for short term studies, and no correlation for long term studies. However, it can be noted that the hypothesis is based on a study [27] where short exposure time was defined as 24 weeks, i.e. 6 months and long exposure time defined as 88 weeks, i.e. 22 months. The minimum exposure time in the dataset was equal to 18 months; thus all the specimens would be considered long term with the definition in [27].

In the general data collection, no significant correlation between crack width and corrosion rate is observed; the p-value of the correlation is larger than 0.05, meaning that there is more than a 5 % chance that the observed correlation is the result of chance and the hypothesis of no-correlation is true. This is valid for any extract of the dataset, even when only specimens with exposure time shorter than 36 months were considered (in Appendix).

The absence of correlation between C_w and P_{rate} indicates that part of **H2** holds on the dataset, i.e. for long exposure times, crack width does not influence the corrosion rate.

4.5 H3: Crack width and corrosion area

Hypothesis three says the extent of the corrosion area is independent from surface crack width. **H3** looks hence into the correlation between crack width (C_w) and the length of a corrosion pit (P_l). No correlation is expected between the two parameters, if the hypothesis holds on the dataset.
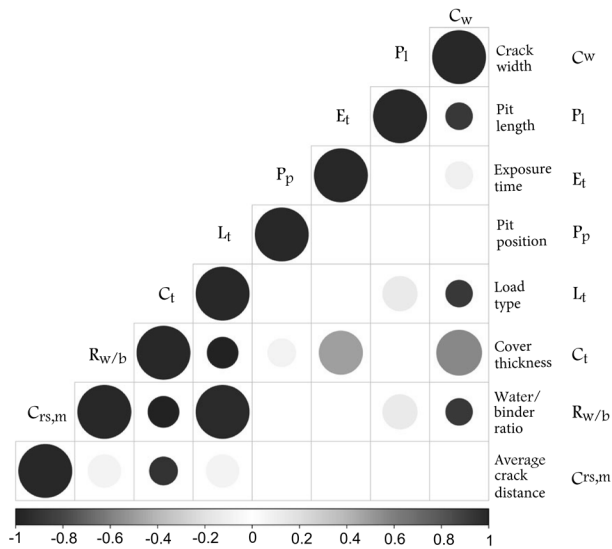
Fig. 7 Representation of the Spearman's coefficient between main parameters in an extract of the dataset where the length of the corroded area is considered. Blank cells correspond to p-values larger than 0.05. Note that the size of the circles increases with the absolute values of ρ

In Fig. 7, the Spearman's coefficient between the main parameters is presented for the data in which measurements of the length of the area containing the corrosion pit are given. In Fig. 7, the crack width (C_w) is negatively correlated with P_l, which is not the expected outcome. This would indicate that, in the dataset considered in this study, smaller crack widths correspond to corrosion pits covering larger areas.

This result does not agree with the expected one of the hypothesis, which would be no correlation. Further, it can be argued that a positive correlation would be more reasonable than a negative, since large surface crack width can intuitively be assumed to correspond to a larger corroded area in correspondence of the pit.

After looking at the correlation between the main parameters, the dataset was checked for possible biases resulting from the experimental configurations. This was done by looking at correlation between experimental choices. In Fig. 7, C_w is shown to correlate with three experimental choices: load type, cover thickness and water/binder ratio. The correlation with load type indicates that smaller crack widths, in the dataset, correspond to statically and cyclically loaded specimens. Loading during exposure is expected to increase the damage area at the steel concrete interface, giving access to the chlorides to a

larger area of the reinforcement bar [26]. If crack width was measured after pre-cracking the specimens, but before exposure (and corresponding loading), the recording of the surface crack width was not affected by the type of loading. Thus, larger slip and separation zones may correspond to smaller surface crack width in the dataset, thus possibly explaining the observed correlation. Additionally, changes in loading conditions during exposure time are expected to directly influence surface crack opening, with crack widths decreasing in unloaded specimens due to the absence of applied loads.

Other observed correlations are increasing crack width with cover thickness, which is expected, as same specimens in the dataset are tested via 3-point bending. Further, lower water/binder ratio corresponds to larger crack width. Low water/binder ratio is generally expected to decrease corrosion rate due to decreased porosity causing, among others, increased resistivity. Also these observed unintended bias of the data provide possible explanations for the contradictory result of this hypothesis.

4.6 H4: Crack width and cover quality

The fourth hypothesis says cover thickness and quality influences the corrosion rate more than surface crack widths do. The hypothesis looks therefore at the correlation between corrosion rate (P_{rate}) and three other parameters: cover thickness (C_t), water/binder ratio ($R_{w/b}$), and crack width (C_w). A negative correlation is expected between P_{rate} and C_t, i.e. the corrosion rate is expected to decrease with the cover thickness. A positive correlation is expected between P_{rate} and $R_{w/b}$, i.e. the corrosion rate is expected to increase with the water/binder of the concrete. Crack width (C_w) was already observed not to have any correlation with corrosion rate (P_{rate}) in the dataset (Figs 5 and 6).

P_{rate} and cover thickness (C_t) were as expected strongly negatively correlated in one extract of the dataset (Fig. 6), but weakly positively correlated in the other (Fig. 5).

$R_{w/b}$ is negatively correlated with P_{rate} in both extracts of the dataset, though only weakly in Fig. 5. This implies that corrosion rate increases with low water/binder ratios, which opposes the formulated hypothesis.

Comparing Figs. 5 and 6 may help explain the observed correlations. Specifically, we are looking at correlations between experimental choices, and possibly at differences between these correlations in the two extracts of the dataset. It is in fact important to observe that the two figures are two different subsets of the dataset, and are therefore based on two different sets of data. The presence of biases in the two subsets could in fact influence the observed correlation between the main parameters.

When looking at the correlation between exposure time E_t and C_t and $R_{w/b}$, it may be noted that the correlation has the same strength, but opposite sign with respect to the correlation the two variables have with P_{rate}. The exposure time is an experimental choice, and so are cover thickness and water/binder ratio, therefore the existence of a correlation can be considered a bias of the dataset. Corrosion rate is calculated from the exposure time, and this appears to result, in Figs. 5 and Fig. 6 in a strong correlation with the parameters the exposure time is correlated with. Even strong correlations are therefore likely to be a result of this bias, and cannot be considered representative of the effect of concrete thickness or water/binder ratio on the corrosion rate.

It is worth observing how corrosion rate (P_{rate}) correlates with exposure time (E_t). Both in Figs. 5 and 6 , P_{rate} and E_t are negatively correlated. P_{rate} is defined as the ratio of the loss of cross-sectional area or the maximum depth of the pit to the exposure time. A strong, negative correlation, as the one observed, indicates that the depth of observed corrosion pits seems to grow slower with time.

In Figs. 5 and 6 , $R_{w/b}$ appears to be positively correlated with the relative position of the pit with respect to a crack (P_p), possibly suggesting that the formation of corrosion pits is less localised at cracks for the case of porous concrete. However, it is as well important to notice that the variability in cover thickness and water/binder ratio in the dataset is limited (see Fig. 1).

The effect of cover quality can be further investigated by looking at Fig. 8. In Fig. 8, the Spearman's coefficient between the main parameters for each reinforcement bar in the dataset is presented. N_{cracks} represents the total number of cracks per meter of bar, and N_{pits} is the number of pits per meter of bar. The number of pits per meter is observed to increase with
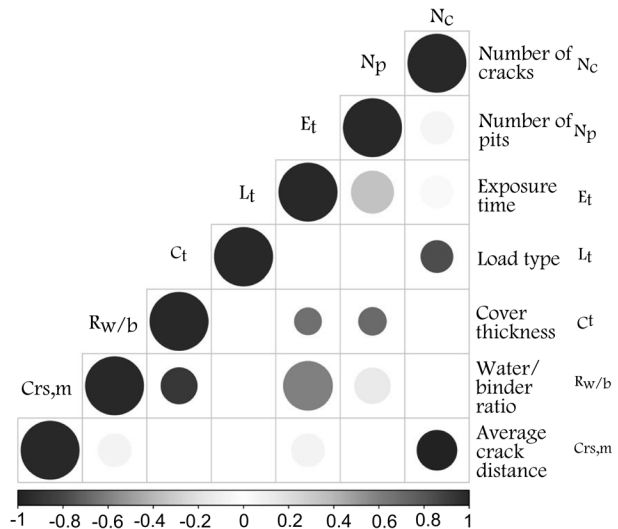

Fig. 8 Representation of the Spearman's coefficient between main parameters for each reinforcement bar in the dataset. Blank cells correspond to p-values larger than 0.05. N_{cracks} represents the total number of cracks per meter of bar, and N_{pits} is the number of pits per meter of bar

$R_{w/b}$ and decrease with increasing C_t. An increase in cover thickness is expected to be beneficial for preventing corrosion damage, while more porous concrete may facilitate the formation of corrosion pits in the case of uncracked concrete. The number of pits is as well observed to increase with corrosion time, which is expected.

To conclude, the impact of cover thickness and quality on the corrosion rate was not possible to assess due to biases in the dataset. However, an increase in cover thickness appears to correspond to a decrease in number of pits per meter of bar, while, when porous concrete is used, corrosion pits may be located further away from transversal cracks. It is also particularly of interest to observe that corrosion pits do not appear to significantly increase in depth with increasing corrosion time. However, they appear to increase in number.

4.7 H5: Crack frequency and corrosion

The fifth hypothesis says that increased crack frequency (smaller crack distance) causes reduced local corrosion rate. This hypothesis thus focuses at the correlation between the average distance between the cracks $C_{rs,m}$ and corrosion rate P_{rate}. In Figs. 5 and 6 , the correlation between the two variables was observed to be negative: corrosion rate decreased

with increasing crack distance (i.e., decreased crack frequency). This result is the opposite of the formulated hypothesis.

Possible biases in the dataset may be observed by looking at how different experimental choices correlate with $C_{rs,m}$. As in Section 4.6, the correlation between $C_{rs,m}$ and E_t appears to be the main reason for the correlation between $C_{rs,m}$ and P_{rate}.

In Fig. 5 and 6 , $C_{rs,m}$ is positively correlated with pit position (P_p), indicating the presence of pits further away from the crack with increasing average crack distance. This may as well be a result of the experimental bias in the dataset between the exposure time and $C_{rs,m}$: specimens with the longest exposure time likely developed corrosion-induced cracks, thus possibly influencing corrosion distribution.

4.8 Recommendations for future experimental work

The observed correlations between experimental configuration parameters described in Section 4.2 represent unintended bias in existing experimental data. It is recommended that future experimental work is designed to address this bias. It is recommended to execute long-term experiments on natural corrosion in pre-cracked specimens in chloride environment, and to carefully document (evolution of) cracks and corrosion characteristics, such as pit locations and characteristics. Note that the weight loss method does not provide sufficient information on the pit characteristics; instead, 3D scanning of rebars after exposure is recommended as a suitable method. Possibly even better would be to use X-ray at several occasions during the exposure time, as this method has potential to follow the evolution of corrosion characteristics (pit growth), see [72] [73]. To reduce the bias indicated in Section 4.2, the design of future experimental series is recommended to focus on:

- Varying exposure time for the same setup. The mentioned use of X-ray during the exposure time has potential to address this lack of data.
- Decoupling the effect of cover thickness and crack spacing by combining large concrete cover with small average crack spacing, and small concrete cover with large average crack spacing.
- Decoupling the effect of concrete quality and crack spacing by combining good concrete quality and small average crack spacing, and low concrete quality and large average crack spacing.

To obtain the desired combinations of e.g. large concrete cover and small average crack spacing, careful design of the specimen geometry, reinforcement ratio, reinforcement diameter, and loading mechanisms is required, possibly also loading including combined bending and tensile load.

Finally, the measurement of surface crack width deserves commenting, as different measurement methods were used in the studies described. The following choices may affect these measurements: when measurements are done, on wet or dry specimens, at different locations, and with different instruments. Standard definitions of what the surface crack width is and how it should be measured would certainly be helpful. In absence of such definitions, we recommend to measure at several times before, during and at the end of exposure, and to clearly define the procedures chosen.

5 Conclusions

In this work, a compilation of data from literature on corroded reinforced concrete specimens exposed to chloride environments is presented. All of the specimens were pre-cracked in 3-point bending and exposed to solutions of water and salt. Five hypotheses on the effect of transversal cracks on corrosion characteristics were formulated based on literature findings. Statistical methods were used to test the hypotheses on the collected dataset. The following was observed:

- Corrosion pits typically appeared close to a crack. The closer the pit was to a crack, the higher the average corrosion rate of the pit.
- In general, no correlation between crack width and average corrosion rate was observed, neither in long- nor short-term experiments.
- In the dataset, smaller crack widths surprisingly correspond to larger pit lengths. This is probably due to unintended bias in the dataset, e.g. that statically and cyclically loaded specimens happened to have smaller crack widths than unloaded specimens.

- The depth of corrosion pits seem to grow slower and slower with time. In contrast, the number of corrosion pits per meter was observed to increase with time. This may be related to a higher chloride concentration in the concrete with time, and/or the appearance of corrosion-induced cracks.
- Results point out discrepancies in the type of data collected by different researchers, arguing for the need of clearly defined procedures for the assessment of crack openings and corrosion damage.

Finally, it can be concluded that the availability of experimental data was relatively scarce, and included some unintended bias. More, well-documented experiments on naturally corroded concrete structures exposed to chloride environments are needed to improve our understanding, and possibly for developing new guidelines for corrosion prevention. The statistical analysis was used to identify bias in the existing data. This was compiled in the form of recommendations for future experimental work required to reduce the bias.

Declarations

Conflict of interest The authors declare that they have no known competing financial interests or personal relationships that could have appeared to influence the work reported in this paper.
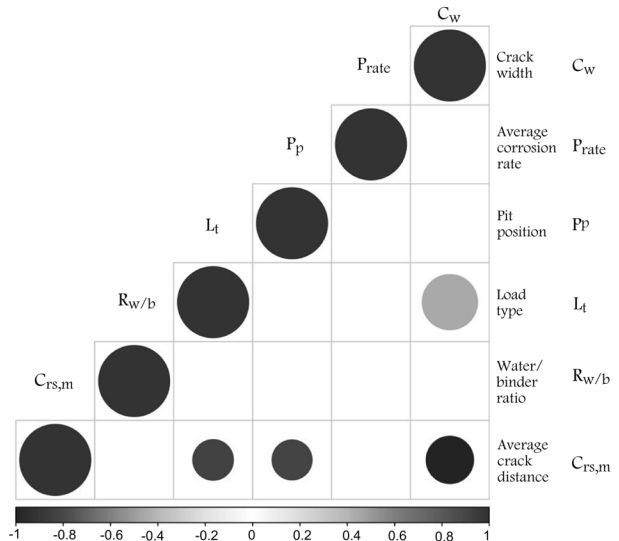
Fig. 9 Representation of the Spearman's coefficient between various parameters in an extract of the dataset where the surface of the pit is used to calculate corrosion rate. Blank cells correspond to p-values larger than 0.05
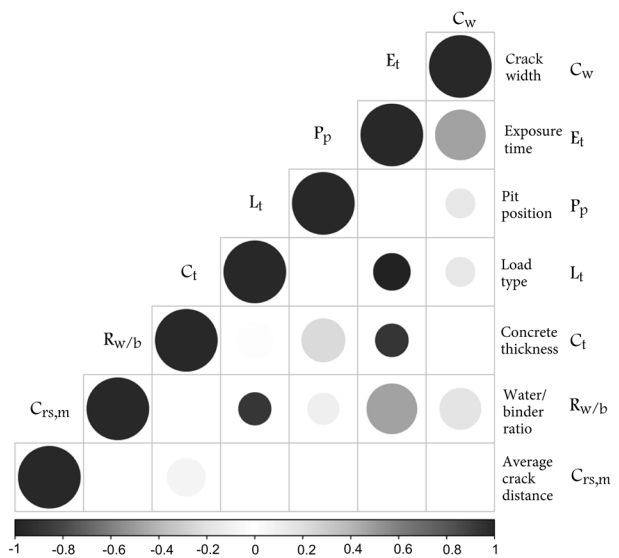

Fig. 10 Representation of the Spearman's coefficient between various parameters in an extract of the dataset where no corrosion cracks are present. Blank cells correspond to p-values larger than 0.05

Fig. 11 Representation of the Spearman's coefficient between various parameters in an extract of the dataset where corrosion cracks are present. Blank cells correspond to p-values larger than 0.05
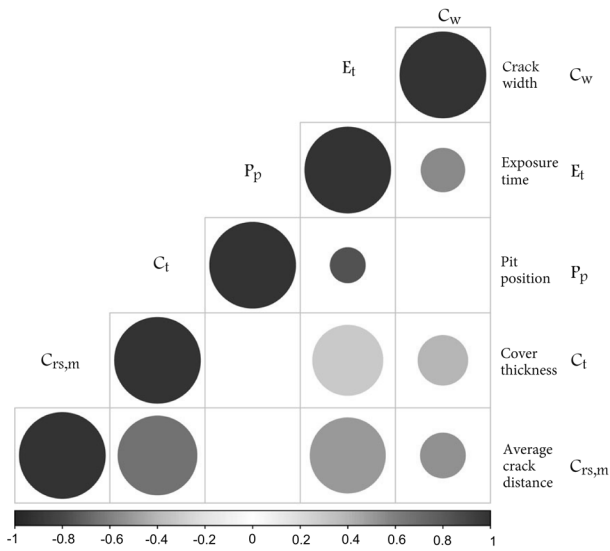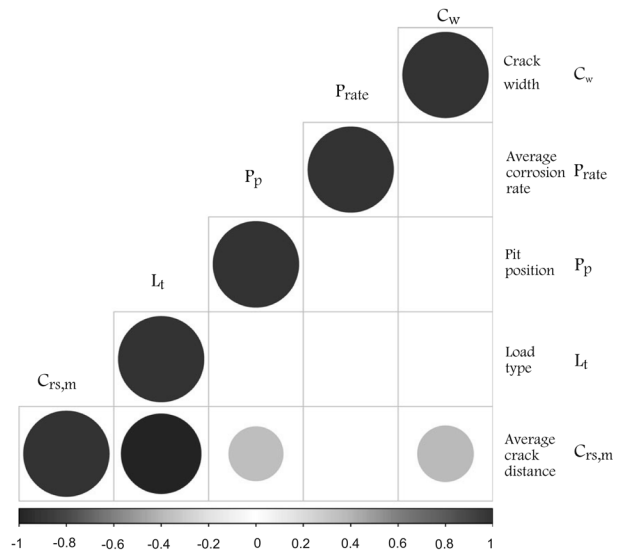

Fig. 12 Representation of the Spearman's coefficient between various parameters in an extract of the dataset where only specimens with short exposure time are selected. Corrosion rate is calculated from the maximum loss of cross sectional area. Blank cells correspond to p-values larger than 0.05

Fig. 13 Representation of the Spearman's coefficient between various parameters in an extract of the dataset where only specimens with short exposure time are selected. Corrosion rate is calculated from the maximum depth of the pit. Blank cells correspond to p-values larger than 0.05
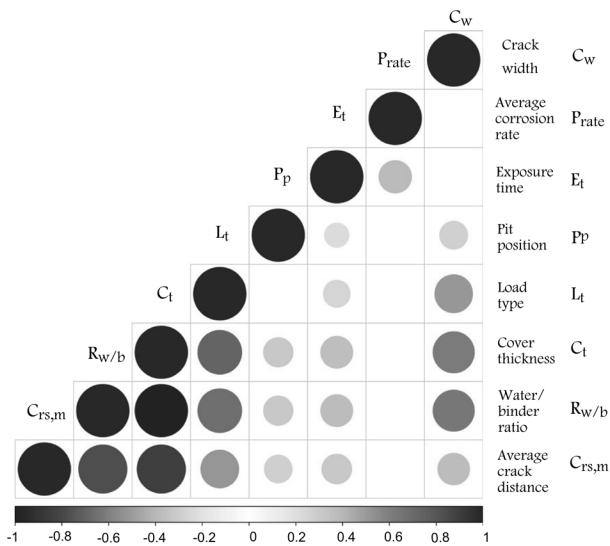
Appendix

In this section, different extracts of the dataset are presented, to complement those shown in the main article.
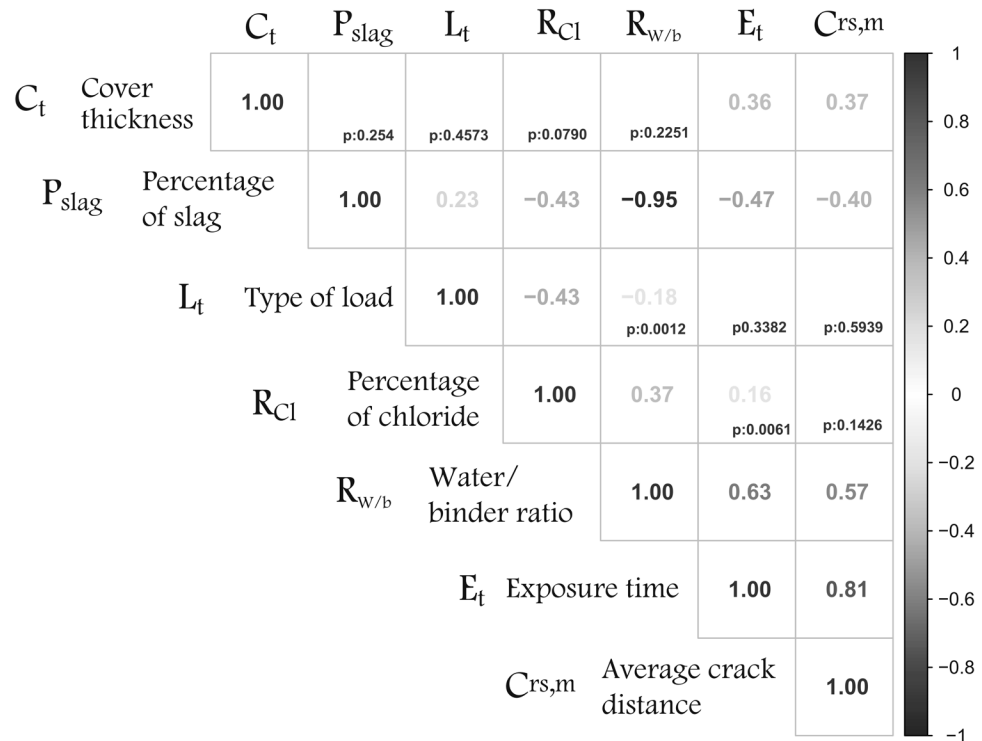
In Fig. 9, the Spearman's coefficient between the main parameters is presented for data in which corrosion rate is measured based on the surface area of the pit.

In Fig. 10, the Spearman's coefficient between the main parameters is presented for data collected from specimens in which no corrosion-induced cracks are present.

In Fig. 11, the Spearman's coefficient between various parameters is presented for data collected from specimens in which corrosion-induced cracks are present.

In Fig. 12, the Spearman's coefficient between the various parameters is presented for data collected from specimens exposed to an environment with chlorides

Fig. 14 Representation of the Pearson's coefficient between experimental parameter. Blank cells correspond to p-values larger than 0.05

		C_t	P_{slag}	L_t	R_{Cl}	$R_{w/b}$	E_t	$C_{rs,m}$
C_t	Cover thickness	1.00	p:0.254	p:0.4573	p:0.0790	p:0.2251	0.36	0.37
P_{slag}	Percentage of slag		1.00	0.23	−0.43	**−0.95**	−0.47	−0.40
L_t	Type of load			1.00	−0.43 (p:0.0012)	−0.18 (p0.3382)	(p:0.5939)	
R_{Cl}	Percentage of chloride				1.00	0.37	0.16 (p:0.0061)	(p:0.1426)
$R_{w/b}$	Water/binder ratio					1.00	0.63	0.57
E_t	Exposure time						1.00	0.81
$C_{rs,m}$	Average crack distance							1.00

for less than 36 months. Corrosion rate is defined as the ratio between the maximum loss of cross-sectional area in the pit and the total exposure time.

In Fig. 13, the Spearman's coefficient between various parameters is presented for data collected from specimens exposed to an environment with chlorides for less than 36 months. Corrosion rate is defined as the ratio between the maximum depth of the pit and the total exposure time.

In Fig. 14, the Pearson's coefficient between various experimental choices is presented together with the associated p-values. In table the corresponding p values are given.

References

1. Bell B (2004) European Railway Bridge Problems. Sustain brid 1:3
2. Andrade C (2018) Some historical notes on the research in corrosion of reinforcement. Hormigón y Acero 69:21–28. https://doi.org/10.1016/j.hya.2018.12.002
3. Tuutti K (1982) Corrosion of steel in concrete. Tech. rep, Swedish Cement and Concrete Research Institute, Stockholm
4. Beeby AW (1979) Prediction of crack widths in hardened concrete. Struct Eng 57A(1):9–17
5. Haynes HH, Abolitz AL, Anderson AR, Boaz I, Boyd AD, Cichanski WJ, Clarke J, Dobrowolski JA, Duncan JM, Litton RW, Mattock AH, Runge KH, Smith CE, Smith RJ, Stiansen SG, Yee AA, Monnier TH Guide for the Design and Construction of Fixed Offshore Concrete Structures. https://doi.org/10.14359/10516
6. CEN, EN 1992-1-1:2004: E, (2004). http://link.springer.com/10.1007/978-3-642-41714-6_51753
7. Käthler CB, Angst UM, Hornbostel K, Elsener B (2020) Critical analysis of experiments on reinforcing bar corrosion in cracked concrete. ACI Mater J 117(3):145–154. https://doi.org/10.14359/51722408
8. Chen E, Berrocal CG, Löfgren I, Lundgren K (2020) Correlation between concrete cracks and corrosion characteristics of steel reinforcement in pre-cracked plain and fibre-reinforced concrete beams. Mater Struct Mater Construct 53(2):1–22. https://doi.org/10.1617/s11527-020-01466-z
9. Jiménez-Quero V, Montes-García P, Bremner T (2010) Influence of concrete cracking on the corrosion of steel reinforcement, 2010 concrete under Severe Conditions: Environment and Loading - Proceedings of the 6th International Conference on Concrete under Severe Conditions, pp. 383–389
10. Mohammed TU, Otsuki N, Hisada M, Shibata T (2001) Effect of crack width and bar types on corrosionof steel in concrete. J Mater Civ Eng 13(3):194–201. https://doi.org/10.1061/(asce)0899-1561(2001)13:3(194)
11. Boschmann Kathler A, Angst U, Wagner M, Larsen C, Elsener B (2017) Effect of cracks on chloride- induced corrosion of steel in concrete - a review. Int Corros Process 41:1–23
12. Danner T, Jakobsen UH, Geiker MR (2019) Mineralogical sequence of self-healing products in cracked marine

concrete. Minerals 9(5):284–289. https://doi.org/10.3390/min9050284

13. Angst UM, Geiker MR, Alonso MC, Polder R, Isgor OB, Elsener B, Wong H, Michel A, Hornbostel K, Gehlen C, François R, Sanchez M, Criado M, Sørensen H, Hansson C, Pillai R, Mundra S, Gulikers J, Raupach M, Pacheco J, Sagüés A The effect of the steel-concrete interface on chloride-induced corrosion initiation in concrete: a critical review by RILEM TC 262-SCI, Materials and Structures/Materiaux et Constructions 52(4). https://doi.org/10.1617/s11527-019-1387-0

14. Lopez-Calvo HZ, Montes-García P, Jiménez-Quero VG, Gómez-Barranco H, Bremner TW, Thomas MD (2018) Influence of crack width, cover depth and concrete quality on corrosion of steel in HPC containing corrosion inhibiting admixtures and fly ash. Cement Concrete Compos 88:200–210. https://doi.org/10.1016/j.cemconcomp.2018.01.016

15. Geiker M, Danner T, Michel A, Belda Revert A, Linderoth O, Hornbostel K (2021) 25 Years of field exposure of pre-cracked concrete beams; combined impact of spacers and cracks on reinforcement corrosion. Construct Build Mater 286:122–801. https://doi.org/10.1016/j.conbuildmat.2021.122801

16. Blagojevic A (2016) The Influence of Cracks on the Durability and Service Life of Reinforced Concrete Structures in relation to Chloride-Induced Corrosion, Ph.D. thesis

17. Šavija B, Schlangen E (2016) Autogeneous healing and chloride ingress in cracked concrete. Heron 61(1):15–32

18. Danner T, Geiker MR (2018) Long-term influence of concrete surface and crack orientation on self-healing and ingress in cracks - field observations. Nordic Concrete Res 58(1):1–16. https://doi.org/10.2478/ncr-2018-0001

19. Tammo K, Thelandersson S (2009) Crack widths near reinforcement bars for beams in bending. Struct Concrete 10(1):27–34. https://doi.org/10.1680/stco.2009.10.1.27

20. Yu L, François R, Dang VH, L'Hostis V, Gagné R (2015) Development of chloride-induced corrosion in pre-cracked RC beams under sustained loading: effect of load-induced cracks, concrete cover, and exposure conditions. Cement Concrete Res 67:246–258. https://doi.org/10.1016/j.cemconres.2014.10.007

21. Otieno M, Beushausen H, Alexander M (2012) Towards incorporating the influence of cover cracking on steel corrosion in RC design codes: the concept of performance-based crack width limits. Mater Struct Mater Construct 45(12):1805–1816. https://doi.org/10.1617/s11527-012-9871-9

22. Pease BJ, Geiker MR (2018) Durability-related crack width and concrete cover requirements and recommendations from reinforced concrete design codes., Tech. rep., Department of Structural Engineering NTNU

23. Hornbostel K, Geiker MR (2017) Influence of cracking on reinforcement corrosion. In: the nordic concrete federation. Oslo, London pp 53–59

24. Bertolini L, Elsener B, Pedeferri P, Polder R (2004) Corrosion of steel in Concrete. Repair., Weinheiim, Germany, Prevention, Diagnosis

25. Tammo K, Thelandersson S (2006) Crack opening near reinforcement bars in concrete structures. Struct Concrete 7(4):137–143. https://doi.org/10.1680/stco.2006.7.4.137

26. Michel A, Solgaard AO, Pease BJ, Geiker MR, Stang H, Olesen JF (2013) Experimental investigation of the relation between damage at the concrete-steel interface and initiation of reinforcement corrosion in plain and fibre reinforced concrete. Corros Sci 77:308–321. https://doi.org/10.1016/j.corsci.2013.08.019

27. Schießl P, Raupach M (1997) Laboratory studies and calculations on the influence of crack width on chloride-induced corrosion of steel in concrete. ACI Mater J 94(1):56–62. https://doi.org/10.14359/285

28. Li W, Liu W, Wang S (2017) The effect of crack width on chloride-induced corrosion of steel in concrete. Adv Mater Sci Eng. https://doi.org/10.1155/2017/3968578

29. François R, Arliguie G (1999) Effect of microcracking and cracking on the development of corrosion in reinforced concrete members. Magaz Concrete Res 51(2):143–150. https://doi.org/10.1680/macr.1999.51.2.143

30. François R, Khan I, Vu NA, Mercado H, Castel A (2012) Study of the impact of localised cracks on the corrosion mechanism. Europ J Environ Civ Eng 16(3–4):392–401. https://doi.org/10.1080/19648189.2012.667982

31. Tammo K, Thelandersson S (2009) Crack behavior near reinforcing bars in concrete structures. ACI Struct J 106(3):259–267

32. Pease B, Geiker M, Stang H, Weiss J (2011) The design of an instrumented rebar for assessment of corrosion in cracked reinforced concrete. Mater Struct Mater Construct 44(7):1259–1271. https://doi.org/10.1617/s11527-010-9698-1

33. Otieno M, Beushausen H, Alexander M (2016) Chloride-induced corrosion of steel in cracked concrete - part I: experimental studies under accelerated and natural marine environments. Cement Concrete Res 79:373–385. https://doi.org/10.1016/j.cemconres.2015.08.009

34. Scott A, Alexander MG (2007) The influence of binder type, cracking and cover on corrosion rates of steel in chloride-contaminated concrete. Magaz Conc Res 59(7):495–505. https://doi.org/10.1680/macr.2007.59.7.495

35. Otieno MB, Alexander MG, Beushausen HD (2010) Corrosion in cracked and uncracked concrete - influence of crack width, concrete quality and crack reopening. Magaz Concrete Res 62(6):393–404. https://doi.org/10.1680/macr.2010.62.6.393

36. Alexander MG, Beushausen H, Otieno MB (2012) Research Monograph no 9: corrosion of steel in reinforced concrete: influence of binder type, water/binder ratio, cover and cracking, department of civil engineering. Univ Cape Town Concrete Mater Struct Integr Res Unit (CoMSIRU) 10(9):4–32

37. Jaffer SJ (2007) The influence of loading on the corrosion of steel in cracked ordinary portland cement and high performance concretes, Ph.D. thesis

38. Poursaee A, Hansson CM (2009) Potential pitfalls in assessing chloride-induced corrosion of steel in concrete. Cement Concrete Res 39(5):391–400. https://doi.org/10.1016/j.cemconres.2009.01.015

39. Francois R, Arliguie G, Bardy D (1994) Electrode potential measurements of concrete reinforcement for corrosion evaluation. Cement Concrete Res 24(3):401–412. https://doi.org/10.1016/0008-8846(94)90127-9

40. Francois R, Maso J (1988) Effect of damage in reinforced concrete on carbonation or chloride penetration. Cement Concrete Compos 18(6):961–970

41. Yu L, François R, Dang VH, L'Hostis V, Gagné R (2015) Structural performance of RC beams damaged by natural corrosion under sustained loading in a chloride environment. Eng Struct 96:30–40. https://doi.org/10.1016/j.engstruct.2015.04.001

42. Zhang W, Yu L, François R (2019) Influence of top-casting-induced defects on the corrosion of the compressive reinforcement of naturally corroded beams under sustained loading. Construct Build Mater 229:116912. https://doi.org/10.1016/j.conbuildmat.2019.116912

43. Zhang W, François R, Yu L (2020) Influence of load-induced cracks coupled or not with top-casting-induced defects on the corrosion of the longitudinal tensile reinforcement of naturally corroded beams exposed to chloride environment under sustained loading. Cement Concrete Res 129(January):105972. https://doi.org/10.1016/j.cemconres.2020.105972

44. Zhu W, François R, Zhang C, Zhang D (2018) Propagation of corrosion-induced cracks of the RC beam exposed to marine environment under sustained load for a period of 26 years. Cement Concrete Res 103(April 2017):66–76. https://doi.org/10.1016/j.cemconres.2017.09.014

45. Zhu W, François R, Liu Y (2017) Propagation of corrosion and corrosion patterns of bars embedded in RC beams stored in chloride environment for various periods. Construct Build Mater 145:147–156. https://doi.org/10.1016/j.conbuildmat.2017.03.210

46. Zhu W, François R (2014) Corrosion of the reinforcement and its influence on the residual structural performance of a 26-year-old corroded RC beam. Construct Build Mater 51:461–472. https://doi.org/10.1016/j.conbuildmat.2013.11.015

47. Zhu W, François R, Coronelli D, Cleland D (2013) Effect of corrosion of reinforcement on the mechanical behaviour of highly corroded RC beams. Eng Struct 56:544–554. https://doi.org/10.1016/j.engstruct.2013.04.017

48. Zhang R, Castel A, François R (2010) Concrete cover cracking with reinforcement corrosion of RC beam during chloride-induced corrosion process. Cement Concrete Res 40(3):415–425. https://doi.org/10.1016/j.cemconres.2009.09.026

49. Castel A, François R, Arliguie G (2000) Mechanical behaviour of corroded reinforced concrete beams - Part 1: experimental study of corroded beams. Mater Struct Materi Construct 33(9):539–544. https://doi.org/10.1007/bf02480533

50. Castel A, Vidal T, François R, Arliguie G (2003) Influence of steel - concrete interface quality on reinforcement corrosion induced by chlorides. Magaz Concrete Res 55(2):151–159. https://doi.org/10.1680/macr.2003.55.2.151

51. Zhang R, Castel A, François R (2009) Serviceability Limit State criteria based on steel-concrete bond loss for corroded reinforced concrete in chloride environment. Mater Struct Mater Construct 42(10):1407–1421. https://doi.org/10.1617/s11527-008-9460-0

52. Yu L, François R, Gagné R (2018) Mechanical performance of deep beams damaged by corrosion in a chloride environment. Europ J Environ Civ Eng 22(5):523–545. https://doi.org/10.1080/19648189.2016.1210033

53. Vidal T, Castel A, François R (2004) Analyzing crack width to predict corrosion in reinforced concrete. Cement Concrete Res 34(1):165–174. https://doi.org/10.1016/S0008-8846(03)00246-1

54. Vidal T, Castel A, François R (2007) Corrosion process and structural performance of a 17 year old reinforced concrete beam stored in chloride environment. Cement Concrete Res 37(11):1551–1561. https://doi.org/10.1016/j.cemconres.2007.08.004

55. François R, Castel A, Vidal T, Vu NA (2006) Long term corrosion behavior of reinforced concrete structures in chloride environnement. J De Phys IV JP 136:285–293. https://doi.org/10.1051/jp4:2006136029

56. Khan I, François R, Castel A (2014) Prediction of reinforcement corrosion using corrosion induced cracks width in corroded reinforced concrete beams. Cement Concrete Res 56:84–96. https://doi.org/10.1016/j.cemconres.2013.11.006

57. Khan I, François R, Castel A (2012) Structural performance of a 26-year-old corroded reinforced concrete beam. Europ J Environ Civ Eng 16(3–4):440–449. https://doi.org/10.1080/19648189.2012.667992

58. François R, Khan I, Dang VH (2013) Impact of corrosion on mechanical properties of steel embedded in 27-year-old corroded reinforced concrete beams. Mater Struct Mater Construct 46(6):899–910. https://doi.org/10.1617/s11527-012-9941-z

59. Dang VH, François R (2014) Prediction of ductility factor of corroded reinforced concrete beams exposed to long term aging in chloride environment. Cement Concrete Compos 53:136–147. https://doi.org/10.1016/j.cemconcomp.2014.06.002

60. François R, Arliguie G (1998) Influence of service cracking on reinforcement steel corrosion. J Mater Civ Eng 10(1):14–20. https://doi.org/10.1061/(asce)0899-1561(1998)10:1(14)

61. Zhang W, François R, Yu L (2020) Influence of load-induced cracks coupled or not with top-casting-induced defects on the corrosion of the longitudinal tensile reinforcement of naturally corroded beams exposed to chloride environment under sustained loading. Cement Concrete Res 129(January):105972. https://doi.org/10.1016/j.cemconres.2020.105972

62. Chen E, Berrocal CG, Fernandez I, Löfgren I, Lundgren K (2020) Assessment of the mechanical behaviour of reinforcement bars with localised pitting corrosion by digital image correlation. Eng Struct 219(June):110936. https://doi.org/10.1016/j.engstruct.2020.110936

63. Edvardsen C (1999) Water permeability and autogenous healing of cracks in concrete. ACI Mater J 96(4):448–454. https://doi.org/10.14359/645

64. Berrocal CG, Löfgren I, Lundgren K (2018) The effect of fibres on steel bar corrosion and flexural behaviour of corroded RC beams. Eng Struct 163(May 2017):409–425. https://doi.org/10.1016/j.engstruct.2018.02.068

65. Zhu W, François R (2015) Structural performance of RC beams in relation with the corroded period in chloride environment. Mater Struct Mater Construct

48(6):1757–1769. https://doi.org/10.1617/s11527-014-0270-2

66. Lee Rodgers J, Alan Nice Wander W (1988) Thirteen ways to look at the correlation coefficient. Am Statist 42(1):59–66. https://doi.org/10.1080/00031305.1988.10475524

67. Chen PY, Popovich PM (2011) Correlation: parametric and nonparametric measures. https://doi.org/10.4135/9781412983808.n1

68. Taylor JR (1997) An introduction to error analysis. University science books, New Jersey

69. Box GEP, Cox DR (1964) An analysis of transformations. J Royal Statist Soc 26(2):211–252. https://doi.org/10.1080/01621459.1981.10477649

70. Dodge Y (2010) The concise encyclopedia of statistics. Springer, London

71. Suzuki K (1990) Mechanism of steel corrosion in cracked concrete. Corros Reinforce oncrete 1:19–28

72. Michel A, Pease BJ, Geiker MR, Stang H, Olesen JF (2011) Monitoring reinforcement corrosion and corrosion-induced cracking using non-destructive x-ray attenuation measurements. Cement Concrete Res 21:1085–1094. https://doi.org/10.1016/j.cemconres.2011.06.006

73. Van Steen C, Pahlavan L, Wevers M, Verstrynge E (2019) Localisation and characterisation of corrosion damage in reinforced concrete by means of acoustic emission and X-ray computed tomography. Construct Build Mater 197(2):21–29. https://doi.org/10.1016/j.conbuildmat.2018.11.159